CONF-800644--7





# OBSERVATION OF DISLOCATIONS AND TWINS IN EXPLOSIVELY COMPACTED ALUMINA

C. S. YUST
L. A. HARRIS

Metals and Ceramics Division
Oak Ridge National Laboratory
Oak Ridge, Tennessee 37830, U.S.A.



*The microstructure at the half-radius position of a polycrystalline alumina rod formed by explosive compaction has been studied by transmission electron microscopy. The as-compacted lattice is composed of differently misoriented bands aligned predominantly in one direction. Such bands may correspond to frequently observed shock lamellae. The band edges are defined by dislocation arrays lying on the basal planes of the hexagonal alumina lattice. The dislocations have Burgers vectors of the type $\{11\bar{2}0\}$ and $\{10\bar{1}0\}$, which are the Burgers vectors of slip dislocations in the basal plane. Basal plane twinning is also observed, and the twin boundaries are found to contain interfacial dislocations. While dislocation generation occurs primarily on basal planes, some dislocation activity is also noted on prism, $\{1\bar{1}00\}$, and on rhombohedral, $\{1\bar{1}01\}$, planes. Nonbasal twinning, however, has not been detected. The lattice damage is discussed in terms of possible dislocation and twinning mechanisms.*

## 1. INTRODUCTION

The use of explosive forces to form, weld, and densify metals has been an active field of endeavor for some time (1,2). The application of such techniques to the compaction of nonmetals, however, is less common. The usual modes of consolidation of ceramic powders have been sintering and hot pressing, and very often additives have been utilized to facilitate densification. These techniques generally yield bodies with residual porosity and retained impurities. The increased demand for full density, high purity ceramics has directed attention to the possibility of alternative fabrication techniques.

## DISCLAIMER

Early work on explosive effects on ceramic powders was directed toward enhancing the sinterability of powders by increased defect content (3,4). Within recent years, efforts have been directed toward consolidation of ceramics by explosive techniques (5). Experiments at Lawrence Livermore Laboratory (LLL) have demonstrated the possibility of ceramic compaction of several ceramics by explosive means (6). This paper is a report of lattice damage observations in an alumina body produced by the LLL workers.

Recent discussions of shock wave effects and associated deformation mechanisms in solids also illustrate the need for more detailed study of such processes. For example, Grady (7) refers to the formation of adiabatic shear zones which cause localized softening or melting, and indicates that little experimental evidence exists for evaluating the relative merits of ductile (i.e., dislocation) and brittle mechanisms of failure (7). The observations reported in this paper provide further background for the understanding of explosive compaction mechanisms in ceramics.

## 2. EXPERIMENTAL

The polycrystalline alumina rod examined in this work was prepared from a tabular alumina powder having a particle size range of 10 to 177 μm. The powder was compacted by enclosing a powder batch, held in a thin-wall steel tube, within a concentric high explosive charge. Ignition of the explosive from one end results in the passage of a shock wave axially along the tube of powder. The resultant alumina rod contained a significant degree of macrocracking but was strong and coherent and had an overall density of 91% of theoretical. Details of the fabrication of this body have already been reported (6).

The powder particles utilized to produce the sample are actually agglomerates of alumina platelets, approximately 6–10 μm thick and 20–30 μm in lateral dimensions, Fig. 1(a). Examination of some of these platelets by transmission electron microscopy shows them to be essentially defect free single crystals. The mass to be compacted, therefore, is an arrangement of small platelets, rather than coherent particles of 10 to 177 μm in size.

The microstructure of this specimen varies with position along the radius, as indicated by both optical and electron microscope examination (8). This investigation is concerned specifically with the microstructural detail at the half-radius position, where the effects of the shock wave on the solid have not been so great that details are obscured by damage density and where thermal effects have been less severe than at the specimen center. At this position in the specimen, areas identified as individual grains by means of optical microscopy correspond in size to many of the original particle agglomerates, Fig. 1(b).

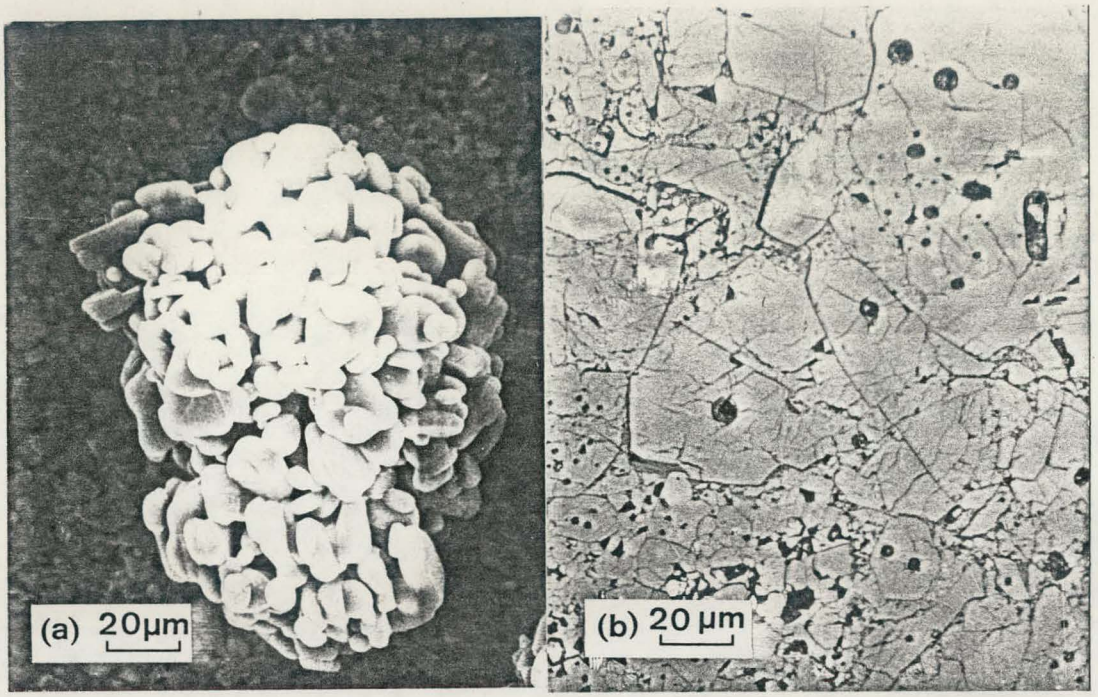


*Figure 1. (a) Scanning electron photomicrograph of the alumina powder particle used to fabricate the sample. (b) The agglomerate of platelets is densified to form the single crystal grains observed in the compacted body by optical microscopy.*

Samples for electron microscope study were prepared from thin slices cut from the sample rod which were ground and polished to 75 µm in thickness, then argon ion milled to electron transparency.

## 3. RESULTS

Observation of the shock-compacted lattice by transmission electron microscopy shows the body to be filled with differently misoriented lattice bands, primarily aligned in one direction, Fig. 2. A more detailed examination of such an area reveals that the lattice consists of arrays of dislocations on basal planes of the hexagonal alumina lattice as well as basal plane twins, Fig. 3. In this view, the basal planes are tilted approximately 40° to the plane of the photo, causing overlap of some of the active planes. Details of the dislocation configurations can be seen, however, even on superimposed planes. The principal features to note are (a) the dislocation arrays lying on successive planes; (b) alternating light and dark fringes along some planes, indicative of a crystallographic boundary; and (c) microcracks or crack precursors formed between some of the active planes.

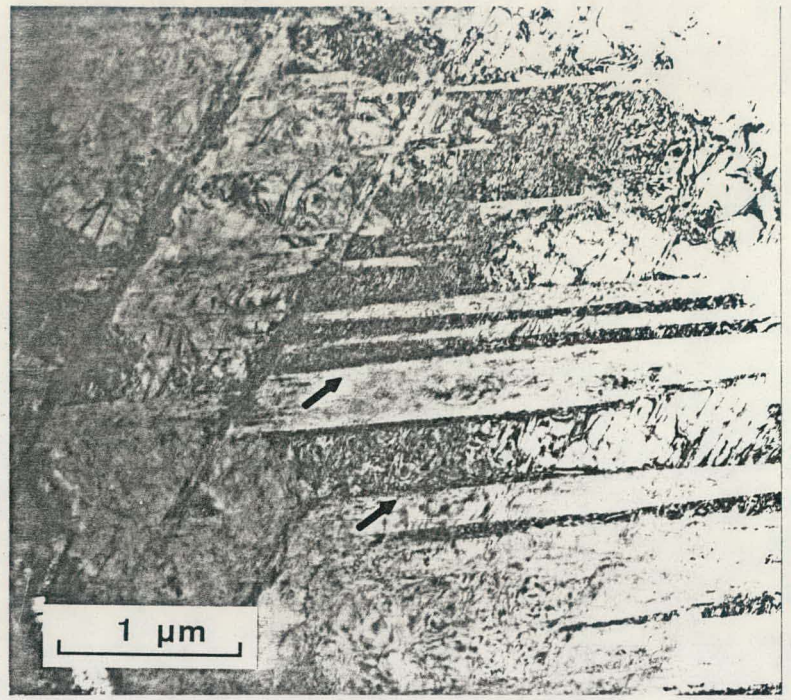


*Figure 2. Transmission electron image of the as-compacted alumina body. Diffraction contrast variations indicate the formation of differently oriented lattice bands, predominatly aligned in one direction, indicated by arrows.*

The dislocations delineated by the bracket "ε" in Fig. 3 are shown in two different imaging conditions in Fig. 4(a) and (b). Some of the dislocation segments visible in Fig. 4(a), where the diffraction vector is $[1\bar{2}10]$, are not observed in Fig. 4(b), and a similar change in visibility of dislocation segments is apparent in Fig. 4(b), where the diffraction vector is $[\bar{3}300]$. Use of this variation of dislocation contrast with imaging conditions permits the identification of the Burgers vector of the dislocations, as shown in Fig. 5. Several of the dislocations in this array exist as pairs, each member of the pair having a Burgers vector of the type $\langle 11\bar{2}0\rangle$, but oriented differently. The paired dislocations, however, are seen to either be formed by or to be forming dislocation segments with a Burgers vector of the type $\langle 10\bar{1}0\rangle$. Five such nodes are present in the "ε" group of dislocations. The pairing of dislocations in this manner is a common feature in this microstructure. Note also that the 1/3 $\langle 11\bar{2}0\rangle$ and $\langle 10\bar{1}0\rangle$ Burgers vectors are the normal Burgers vectors for glide dislocations on the basal plane in alumina (12). The dislocations in Fig. 5 can also be viewed as segments of loops of Burgers vector $\langle 10\bar{1}0\rangle$, possibly emanating from a common source, indicated in the figure as "s."

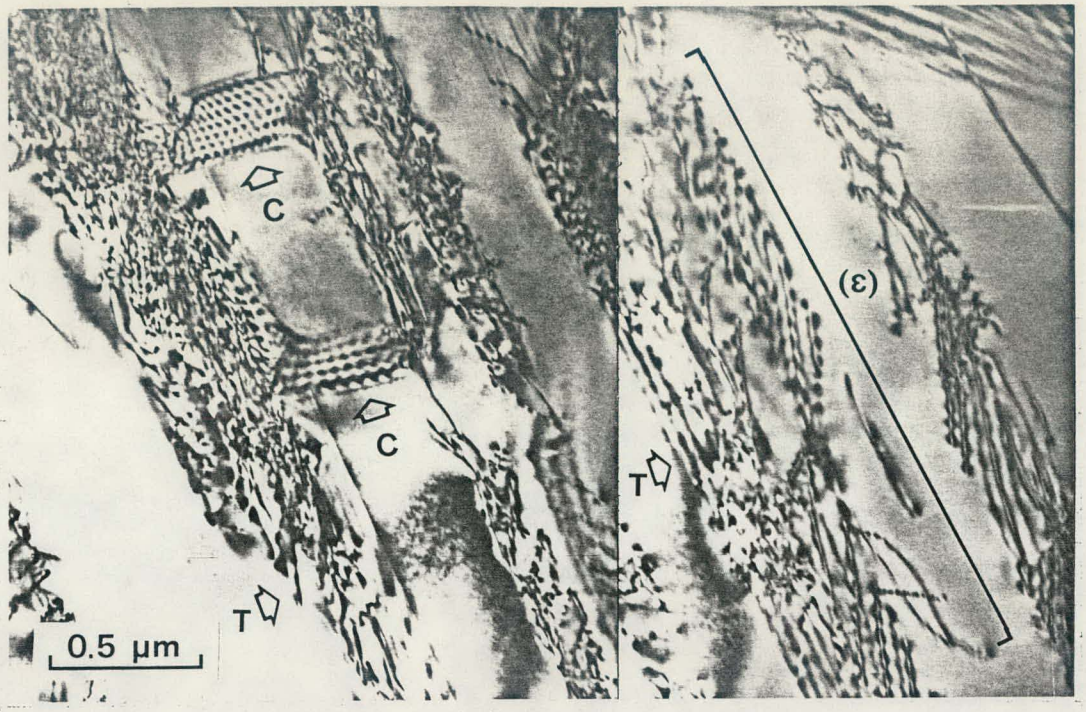


*Figure 3. The differently misoriented lattice bands are separated by parallel dislocation arrays lying on the basal plane. Basal plane twins and microcracks are also formed. Twins are indicated by T, microcracks or crack precursors by C, and a dislocation group studied in further detail by the bracket marked ε. The basal plane is tilted 40° to the plane of the photo.*

The field of view of Fig. 4 can be rotated so that the basal plane is viewed edge-on, Fig. 6. In this position, it is confirmed that the dislocation groups in this region are indeed confined to the basal plane. The imaging condition in this figure is = 0006, a condition for which all dislocations having Burgers vectors lying in the basal plane should be invisible. The Burgers vectors associated with these dislocations do lie in the basal plane, and consequently, the dislocation images should be absent. However, local strain fields around the dislocation locally distort the sample and cause the limited residual contrast seen in Fig. 6. While most of the dislocations are "out of contrast," strong contrast is evident along the lines labeled e, f, g, and h. The origin of the contrast at these lines will be considered when existence of lattice twins is described below.

Observations have also been made of dislocations on the basal plane in parts of the specimen where that basal plane is nearly parallel to the plane of the sample. This orientation permits the inspection of much wider regions of the basal plane, but also suffers the disadvantage of greater overlap of dislocations on

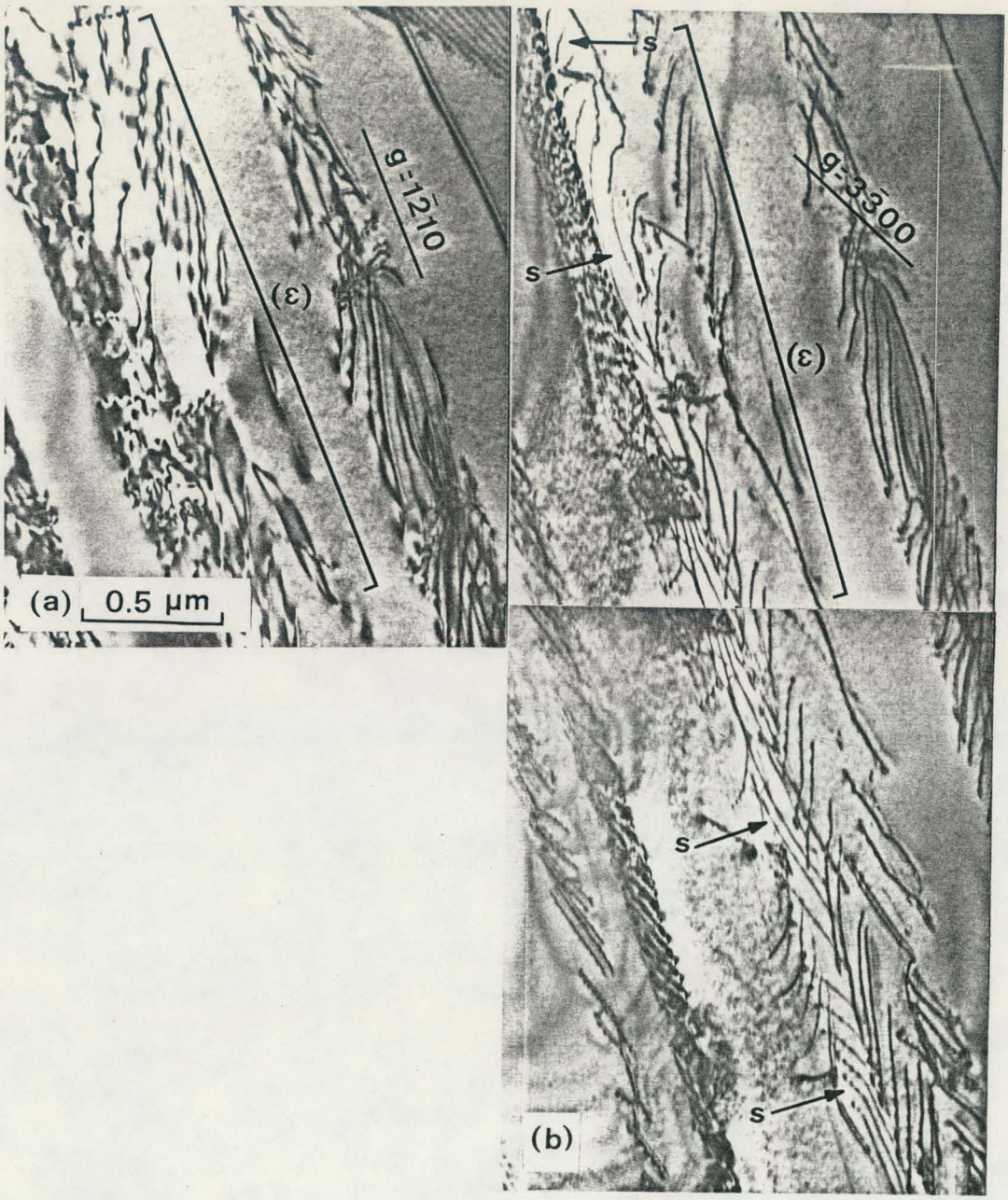


*Figure 4. A portion of the field of Fig. 3(a) as seen in the* $\mathbf{g} = 1\bar{2}10$ *diffraction condition; (b) as seen with* $\mathbf{g} = 3\bar{3}00$. *Comparison of (a) and (b) demonstrates Burgers vector variations. At the left of (b), interfacial dislocations in a twin boundary are seen as sets of loop segments in the boundary, marked* s.

successive planes, Fig. 7. The area shown contains irregular networks superimposed on one another. Evidence of dislocation activity on planes perpendicular to the plane of the photo is present in the diagonal bands, which are the image of dislocation groups lying perpendicular to the plane of the photo. Analysis of such nonbasal arrays indicates that they lie on prism, $\{1\bar{1}00\}$, and on rhombohedral, $\{1\bar{1}01\}$, planes. This observation is consistent with that of Fig. 2 in which it is evident that planes of dislocation activity exist in addition to the basal planes.

Another feature of the shock compacted microstructure is basal plane twinning. Part of the field of Fig. 3 is seen to be a band of distinctly different orientation when tilted to another reflecting condition, Fig. 8, and diffraction analysis shows such a band to be a basal plane twin. The crystallographic elements of the twin are found to be in agreement with those previously determined for basal twinning in alumina. Both Figs. 2 and 7 show that the twin interfaces contain dislocations at the twin boundary. Since these dislocations are contained in the boundary, they may have Burgers

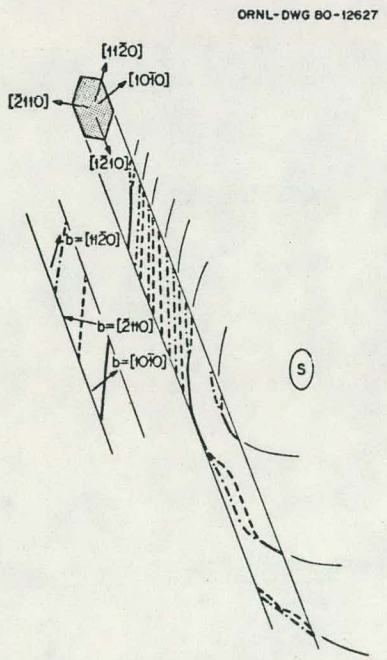


*Figure 5. Schematic view of the dislocation array of Fig. 4; Burgers vector of each dislocation segment is identified through the key, left. 'S' is a possible loop source.*

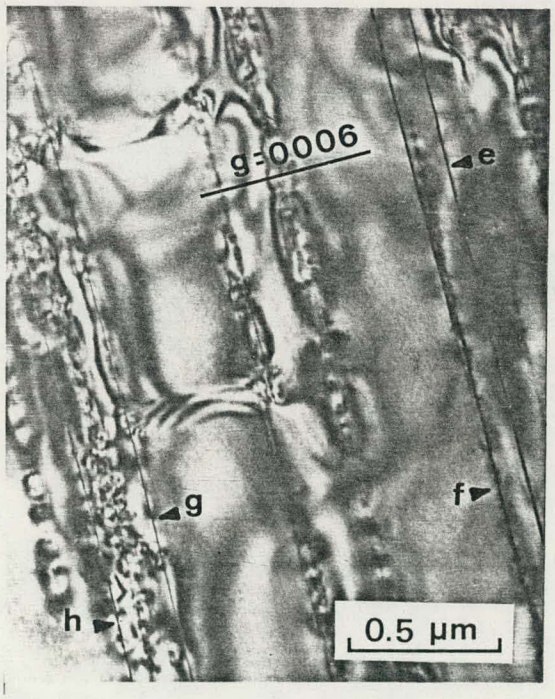


*Figure 6. Field of Figs. 3 and 4 rotated to view the basal plane edge-on. Dislocation generation in this area is confined to the basal plane.*

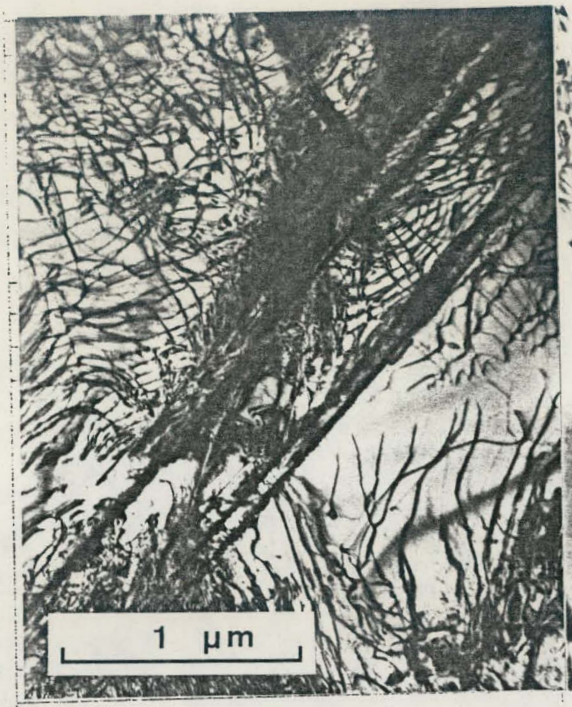


*Figure 7. View of a basal plane nearly parallel to the photo plane. Note large networks and dislocation activity on planes normal to the basal plane.*

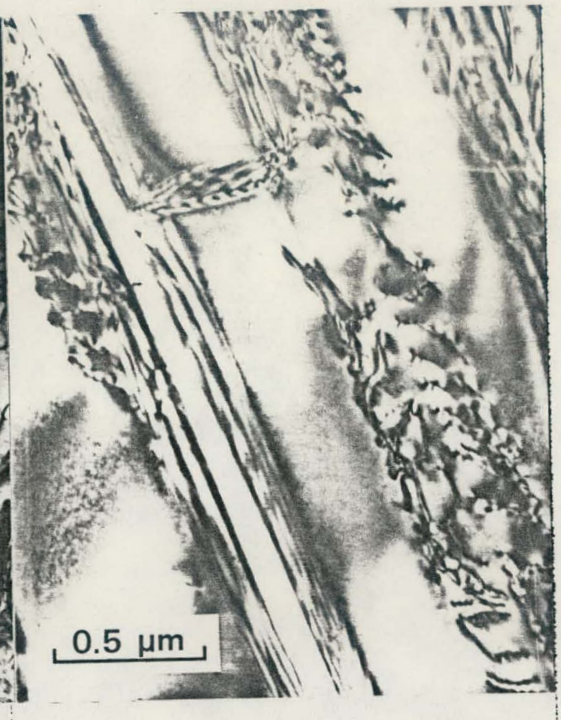


*Figure 8. Part of Fig. 3, tilted to emphasize the contrast at a twin. Boundary fringes and interface dislocations are visible at the border of the twin.*

vectors which are characteristic of the boundary geometry rather than conventional lattice Burgers vectors. If this is the case, such dislocations would remain in contrast in the g = 0006 condition. In Fig. 6, the strong contrast at lines e, f, g, and h is attributed to the nonbasal Burgers vectors of the interfacial dislocations which are present in the twin boundaries.

In some portions of the compacted microstructure, relics of the original particle platelets appear to be identifiable, Fig. 9. The dimensions and general shape of the closely packed contiguous regions seen in Fig. 9 are consistent with that of the agglomerated platelets. In general, the compacted body contains large single crystal volumes much larger in extent than the platelets, see Fig. 1(b). A further piece of evidence testifying to the formation of large single crystal regions from the platelets is found in an optical examination of large grains of the compact by polarized light. Figure 10 shows such a view, focused within the bulk of a single grain, where many small pores are observed to be scattered throughout the mass. This porosity is clearly the remains of the extensive void contained within the platelet mass.

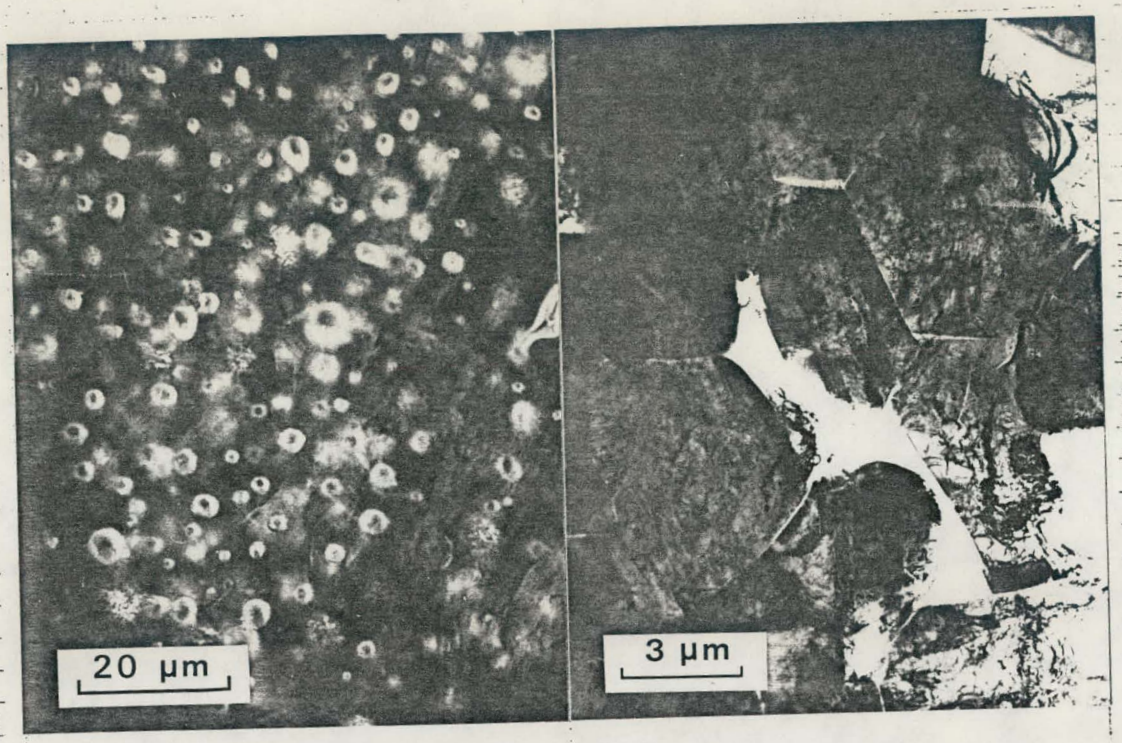


*Figure 9. Relics of the original particle platelets are occasionally observed, although most of the platelets have formed larger crystals.*

*Figure 10. Optical microscopy with polarized light shows the retention of porosity within single grains, also a relic of the platelet agglomerate particle.*

## 4. DISCUSSION

The polycrystalline sample examined in this study has been prepared from a fine particulate mass subjected to intense forces applied at a very high strain rate. The matrix of each particle has experienced the passage of the initial shock and rarefaction waves and, as a consequence of subsequent particle collisions, probably a complex of additional shocks and rarefactions. While the particular stress history for a given point in the solid would be virtually impossible to reconstruct, it is nevertheless useful to consider the details of the microstructure for evidence of the operative deformation mechanisms.

A common observation in recovered samples of shocked minerals, including alumina, is that they contain planar features identified as shock lamellae (7). They have been identified as features separating otherwise undamaged material and as having spacings of 2 to 20 μm. In addition, they are reported to occur on lattice planes of densest packing, and Grady assumes that they correspond to shear zones (7). The observations presented here of dislocation

and twin generation principally on the basal plane, the plane of most dense packing, indicate that shock lamellae probably do have a relationship to deformation zones and yield processes in the shocked crystal lattices.

The stress-strain experience of the deformed matrix is well described by the model developed by Kieffer for Coconino sandstone (9) The model applies specifically to porous, granular media, which is a good representation of the starting agglomerate particle mass considered here. The model is one dimensional, i.e., each particle is represented by a thin slab of infinite extent. The entire particle mass is described as a series of such slabs separated by small gaps representative of the porosity in the body. A shock wave interacting with the particulate mass enters and traverses the first particle. At the first pore a rarefaction wave is transmitted back through the particle as the shock wave is emitted, and the particle accelerates across the pore to strike the second particle. Shock waves are created by the collision in both the first and second particles, moving in opposite directions from the collision interface. The process is repetitive as successive particles interact, resulting in a reverberation of shock and rarefaction waves through the body. Clearly, the stress-strain history at a given point in a three dimensional particulate mass becomes extremely complex.

In the past 20 years, several models have been presented to account for the effects of the interaction of a shock wave with a crystalline lattice. The initial model was that of Smith (2) which described the formation of networks of dislocations at the shock front to alleviate the elastic strain at the shock interface. This model, however, required that the dislocation network move at supersonic velocities with the progressing shock wave. Hornbogen (10) modified the Smith model by introducing the idea of the generation of loops by the shock forces, the edge components of which moved with the shock front, leaving screw segments behind in the lattice. More recently, Meyers (11) has presented a model which utilizes the original Smith concept. Meyers envisions the homogeneous nucleation of a dislocation network to relieve the elastic strain at the shock interface, but once the dislocation wall is formed, the shock wave moves on, leaving the dislocation wall in the lattice. The progressing shock wave again rebuilds the local stress at the shock interface such that another dislocation wall is nucleated. In this manner, the shock wave creates a succession of dislocation walls as it progresses through the lattice. The coincidence between this description and the observation of dislocation arrays on successsive basal planes in the sample of shocked alumina studied here is noteworthy.

The Meyer concept of dislocation formation predicts the homogeneous nucleating of dislocation networks, and therefore the

creation of an array of dislocations having different, or at least differently oriented, Burgers vectors. The dislocation array of Figs. 4 and 5 seem at first inspection to be in accord with this concept, in that most of the dislocations have Burgers vectors of the type $\langle 11\bar{2}0 \rangle$ in one of two orientations. These dislocations, however, are seen to be either joining to form $\langle 10\bar{1}0 \rangle$ type dislocations or splitting from such dislocations. The nominal basal plane dislocation Burgers vectors, $\langle 10\bar{1}0 \rangle$ and $1/3\langle 11\bar{2}0 \rangle$, have respective lengths of 8.22 Å and 4.75 Å (13). Since dislocation self-energy is normally estimated as being proportional to the square of the Burgers vector, the energy balance around the observed dislocation nodes suggests that the $\langle 10\bar{1}0 \rangle$ vectors are decomposing. Snow and Heuer (12) point out that this approximation for self-energy does not necessarily hold for anisotropic materials such as alumina, so that the issue of $\langle 10\bar{1}0 \rangle$ decomposition is not fully resolved, although the large difference in magnitude of the two Burgers vectors involved suggests that the energy estimates are proper and the $\langle 10\bar{1}0 \rangle$ type dislocation forms the $\langle 11\bar{2}0 \rangle$ type dislocations. The agreement with the Meyer model would be more convincing if the $\langle 10\bar{1}0 \rangle$ dislocation segments were not present, or were shown to be forming by combination of the $\langle 11\bar{2}0 \rangle$ segments. In addition, the general form of the dislocation array (Fig. 5), a series of loop segments on the basal plane, is more indicative of the operation of a conventional loop-producing source somewhere on the basal plane, indicated by "s" in Fig. 5, than the homogeneous formation of a network.

The view of the extended basal plane area, Fig. 7, shows evidence of extensive and complex network formation. In this particular field, the basal planes are intersected by prism planes on which dislocations have been formed. The complexity of this dislocation arrangement challenges any effort to identify the origin of the dislocations, but a possible source of dislocations at the intersection of the basal and prism planes is suggested by the shape of the network. The extensive network formation, however, is in accord with the Smith-Meyer models concept of homogeneous network creation.

The potential for microcracking is widely observed in the compacted body, primarily as pre-crack dislocation arrays or as short cracks between successive dislocation layers, as shown in Fig. 3. The dislocation images indicate that significant strain fields exist around the individual dislocations. Presumably these localized stresses at specific dislocation groups can become great enough to nucleate small cracks, some of which grow to significantly larger sizes. It is conceivable that some of the cracks or pre-cracks have formed during thinning for electron microscope examination, but the interrelationship between cracks and dislocations generally observed suggests that most of the micro cracks or pre-crack arrays formed during compaction.

Twinning has also been observed to be an active deformation mechanism in the explosively compacted mass. Twinning is recognized as being favored by high strain rate deformation processes and should be expected in shocked bodies (13,14). Twinning mechanisms are not well defined but can be categorized as either heterogeneous, i.e., involving the generation and motion of dislocations, or homogeneous, i.e., involving lattice shear and associated atomic rearrangement. The observations of this study attest to the fact that dislocations are commonly a part of the twin interface, and imply that dislocation activity is related to the twin creation. For example, the boundary of the twin in plane in Fig. 4(b), is seen to have evidence of three sets of loops in the interface, suggesting 3 loop sources. Each one of these implied sources might be operating in the sense of the pole mechanism described for twin generation (14,15), but the specific features as applied to this particular case are unclear. Since twinning is a very high-rate phenomena, the application of dislocation multiplication mechanisms to twin formation has been recognized as a problem for some time (14).

As shown in Fig. 7, the dislocation activity is not entirely restricted to basal planes, but is predominantly in that system. In view of the arbitrary distribution of intial platelet orientations with respect to the original shock wave, and the complex array of secondary shocks to which mutually impinging particles are subjected, it is not clear why the deformation activity is highly biased toward basal planes. At some point during the compaction process, it would seem likely that shear stresses of sufficient magnitude would be applied to activate secondary slip and twinning systems. On the basis of the geometric preponderance of secondary systems, a greater degree of nonbasal activity would seem to be indicated. Rhombohedral twinnning is common in alumina, for example, but only basal twins have been observed in the course of this work.

A further point for consideration is the actual densification mechanism operating in this compaction. Many of the regions of the densified body which have been studied in this work are large, single crystal regions which retain much, if not all of the mechanical damage experienced during compaction. These regions have somehow formed as coherent areas from the much smaller initial platelets. The mechanism(s) responsible for the observed transformation from polycrystal to single crystal regions is(are) not readily evident to the authors.

## 5. CONCLUSIONS

This investigation of the microstructure of explosively compacted alumina has revealed that both dislocation generation and twin formation are active deformation modes in this densification process. The deformation activity is largely confined to the basal plane, although evidence of dislocation generation on prism planes can be observed. Certain features of the dislocation arrays, such as multiple Burgers vectors and network formation, are in accordance with models of homogeneous dislocation generation, although other features are indicative of the operation of more conventional sources. The specific mechanisms of either dislocation generation or twinning as they occur in explosive compaction are not evident, nor is the mechanism of consolidation of the solid. Microfracturing is observed, and is evidently the consequence of local stresses at dislocation arrays. Many aspects of the process of explosive compaction remain to be clarified.

## 6. ACKNOWLEDGEMENTS

The authors acknowledge their debt to Dr. C. L. Hoenig of Lawrence Livermore Laboratory for providing the sample material, to Mr. L. L. Hall and Mrs. S. B. Waters for skillful preparation of the electron microscope samples on which this work depends, and to Mrs. F. M. Foust for invaluable assistance in the preparation of the manuscript.

The research was sponsored by the Division of Materials Sciences, U.S. Department of Energy, under contract W-7405-eng-26 with the Union Carbide Corporation.

## 7. REFERENCES

1. Pearson, J., "High Energy Rate Working of Metals," Proceedings, NATO Advanced Study Institute, Oslo, Norway, Sept. 1964, pp. 15–37.
2. Smith, C. S., *Trans. Met. Soc. AIME*, 574 (1958).
3. Heckel, R. N., and Youngblood, J. L., *J. Amer. Cer. Soc.*, 51, 398 (1968).
4. Bergmann, O. R., and Barrington, J., *J. Amer. Cer. Soc.*, 49, 502 (1966).
5. Prümmer, R. A., and Ziegler, G., "5th International Conference on High Energy Rate Fabrication, Denver, Colorado, June 24–26, 1975,"
6. Hoenig, C. L., et al., "6th International Conference on High Energy Rate Fabrication, Essen, FRG, Sept. 9–16, 1977,"
7. Grady, D. E., "High-Pressure Research, Applications in Geophysics," p. 389, Academic Press, New York, 1977.

8. Hoenig, C. L., and Yust, C. S., submitted to *Journal of American Ceramic Society*.
9. Kieffer, S. W., *J. Geophys. Res.*, 76, 5449 (1971).
10. Hornbogen, E., *Acta Met.*, 10, 978 (1962).
11. Meyers, M. A., *Scripta Met.*, 12, 21 (1978).
12. Snow, J. D., and Heuer, A. H., *J. Amer. Cer. Soc.*, 56, 153 (1973).
13. Mahajan, S., and Williams, D. F., *Int. Met. Rev.*, 18, 43 (1973).
14. Hirth, J. P., and Lothe, J., "Theory of Dislocations," p. 753, McGraw-Hill, New York, 1968.